



# Photothermal radiometry measurement of thermophysical property change of an ion-irradiated sample

Kyle Horne<sup>a,\*</sup>, Heng Ban<sup>a</sup>, Andreas Mandelis<sup>b</sup>, Anna Matvienko<sup>b</sup>

<sup>a</sup> Mechanical and Aerospace Engineering, Utah State University, Logan, UT 84322, USA

<sup>b</sup> Center for Advanced Diffusion-Wave Technologies (CADIFT), University of Toronto, Toronto M5S3G8, Canada

## ARTICLE INFO

### Article history:

Received 21 March 2011

Received in revised form

26 September 2011

Accepted 31 October 2011

Available online 12 November 2011

### Keywords:

Ceramics

Microanalysis

Photothermal methods

## ABSTRACT

Using photothermal radiometry (PTR) an ion-irradiated ZrC sample's thermal properties are measured by fitting frequency-scan data to a theoretical model for the surface temperature. The technique is shown to measure thermal properties without physical contact of a very small sample.

Published by Elsevier B.V.

## 1. Introduction

Photothermal methods provide an attractive option for nuclear material property measurements, largely since no physical contact is required, small samples can be used, and the sample remains unchanged by the procedure [1]. This allows photothermal methods to be implemented in post-irradiation examination (PIE) applications, and precludes the need for many samples to be prepared for destructive measurements.

The foundation of a photothermal measurement stands upon thermal diffusion waves. By considering the Fourier transform of the heat equation, the frequency response of a thermal system to periodic excitation can be examined. Thermal waves are very diffusive, and only travel a short distance before dispersing. This distance is characterized by the thermal diffusion length  $\mu_j$ , given by Eq. (1), where  $\alpha_j$  is the thermal diffusivity of layer  $j$ :

$$\mu_j = \sqrt{\frac{2\alpha_j}{\omega}} \quad (1)$$

As can be seen from the definition, the thermal diffusion length is dependent on both the angular frequency of excitation  $\omega$ , and the thermal diffusivity of the medium through which the wave passes. This leads to the definition of  $\sigma$  as the thermal wave

number in Eq. (2), where  $i$  is the imaginary unit. Since  $\sigma$  is complex, it expresses both amplitude and phase components of the thermal wave number:

$$\sigma_j = \frac{1+i}{\mu_j} \quad (2)$$

By exciting thermal waves on the surface of a sample and measuring the surface temperature through radiometry, the thermal properties of the sample can be computed [2]. This is due to thermal effects which closely resemble reflection and refraction [3,4].

In this work, the measurement of a proton-irradiated zirconium carbide (ZrC) sample is reported. The properties were measured using photothermal radiometry (PTR), through the use of frequency scans and curve fitting. PTR has previously been proven effective for ceramic samples such as ZrC, although the curve fit process is often restricted to very few degrees of freedom, which has not been done in this study [5–7]. The objective of this study was to examine and demonstrate the feasibility of PTR technique for certain PIE samples, when the irradiation damage is only limited to a thin surface layer ( $\sim 23\text{-}\mu\text{m}$ ). These preliminary results demonstrate the effectiveness of PTR as a potential post-irradiation examination (PIE) technique and suggest that further investigation be done.

## 2. ZrC sample

ZrC is important to nuclear industry because of its potential as a material for advanced nuclear fuels. Because of this and the available data it was selected as the prototypical sample material. The sample was 500- $\mu\text{m}$  thick, with two distinct layers of material

\* Corresponding author. Tel.: +1 435 232 9575; fax: +1 435 797 2417.  
E-mail addresses: [kyle.horne@aggiemail.usu.edu](mailto:kyle.horne@aggiemail.usu.edu), [horne.kyle@gmail.com](mailto:horne.kyle@gmail.com) (K. Horne), [heng.ban@usu.edu](mailto:heng.ban@usu.edu) (H. Ban), [mandelis@mie.utoronto.ca](mailto:mandelis@mie.utoronto.ca) (A. Mandelis), [ann@mie.utoronto.ca](mailto:ann@mie.utoronto.ca) (A. Matvienko).

### Nomenclature

$\mu$	thermal diffusion length
$\alpha$	thermal diffusivity
$\omega$	angular frequency of modulation
$i$	layer index (subscript)
$\sigma$	thermal-wave number
$j$	layer index (subscript)
$i$	imaginary constant
$\delta$	beam radius
$\ominus$	complex surface temperature
$F$	mean beam intensity
$k$	thermal conductivity
$L$	layer thickness
$R$	sample–environment interaction coefficient
$\rho$	layer interaction coefficient
$b$	ratio of thermal effusivities
$C_p$	specific heat
$e_f$	thermal effusivity

which have been damaged by proton bombardment to 1.75 displacements per atom (dpa) at 600 °C. The stoichiometry of the ZrC sample was approximately one, and the sample was not actively releasing radiation.

By irradiating the sample its thermal properties changed to form three major layers in the structure. The first layer is merely damaged by the radiation, but the protons have not embedded. This layer is 23- $\mu\text{m}$  thick. The next layer is only 5- $\mu\text{m}$  thick, but contains the embedded protons as well as lattice damage. The third and final layer is undamaged. The layer thickness estimations are taken from SRIM calculations done by the lab which provided the irradiated sample [8]. These layers are not definite regions with constant properties, but for this study they are treated as such to make the curve-fit results more stable. Therefore, the PTR measurement reflects an averaged value for each layer.

The layered structure of the sample causes thermal waves induced at the surface to be out of phase with the heat flux creating the waves. It is predominantly this phase lag which allows the thermal properties of the sample to be measured using the PTR method.

This particular sample serves as a prototypical sample for PIE. Irradiation experiments with proton or other ion sources often produce small, layered samples which are ideally suited for PTR measurement. For PIE applications, small samples are especially desirable in the case of radioactive materials, since the small size dramatically improves the safety of handling the sample. Additionally, because most accelerators have limited space for sample irradiation, small sample sizes are preferred.

### 3. Experimental methods

Fig. 1 represents the experimental setup used to measure the ZrC sample's photothermal response. A 629 nm laser diode with sinusoidally modulated intensity excites thermal waves on the sample's surface at a particular frequency, directed by the lock-in amplifier through the laser controller. Using the dielectric constants for ZrC in the 629 nm range the extinction coefficient was computed, which predicts a penetration depth on the order of 50 nm [9]. Therefore, metal film was not required for the laser to heat the sample and the thermal waves can be practically treated as originating from the sample's surface. The sample's heated surface emits added infrared radiation which is collected and focused by paraboloidal mirrors to a mercury cadmium telluride (MCT) detector with a 1 mm<sup>2</sup> collection area, the signal of which passes through a pre-amplifier and

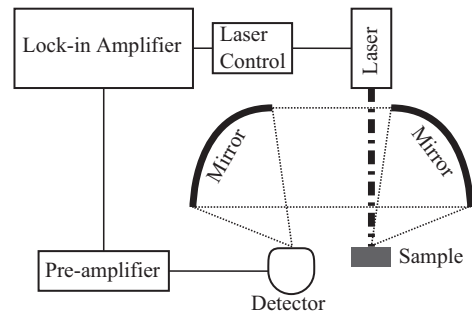


Fig. 1. PTR setup.

on to the lock-in amplifier. The lock-in amplifier is controlled by a computer using National Instruments LabView for which a virtual interface (VI) has been written which runs the frequency scans and records the data. The PTR system used was build previously for other research [10].

The sample was scanned using a laser power on the order of 100 mW and 63% of the beam's intensity was contained within a circle 322  $\mu\text{m}$  in diameter. The beam's diameter was measured by moving a photo detector with a 50- $\mu\text{m}$  aperture across the stage and measuring the beam intensity, as shown in Fig. 2. A Gaussian lineshape was fitted to this profile and the resulting standard deviation from the fit was taken as the beam radius,  $\delta$ .

The ZrC sample was scanned from 500 Hz to 5000 Hz using the LabView interface. Fifteen actual readings were taken at each frequency, but only the last ten were averaged together for the actual measurement; the standard deviation from this average among the last ten samples was also computed. The first five readings are dropped because it takes some time for the thermal system to achieve a stable periodic state.

A glassy carbon sample with known properties was also scanned at the same frequencies in order to obtain the transfer function of the system as configured. The carbon sample is part of the PTR setup in Toronto [10]. The raw data for the sample function is multiplied by the transfer function to remove bias from the system at each frequency, and convert the measured voltages into effective temperatures. This allows the transformed data to be fit against the analytical model.

### 4. Fundamental theory

The gathered data must undergo several computational processes in order to obtain the desired properties. The first step is to convert the measured voltages into equivalent surface

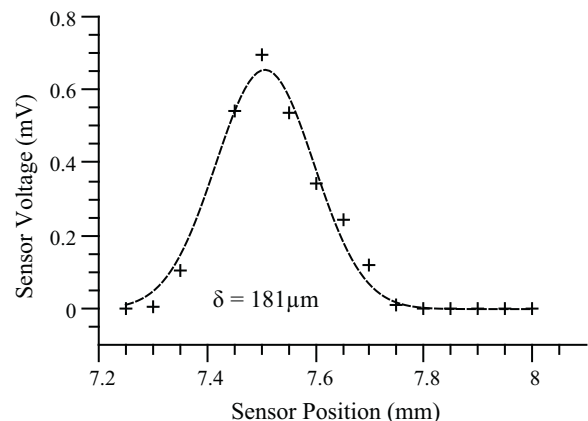


Fig. 2. Laser beam intensity profile.

**Table 1**  
Thermal properties of irradiated ZrC at room temperature [15,16].

Property	Layer I	Layer II	Bulk	Units
Layer thickness $L$	~23	~5	~470	$\mu\text{m}$
Thermal conductivity $k$	10.4	10.0	20.5	$\text{W}/(\text{m K})$
Thermal diffusivity $\alpha$	1.95	6.95	8.88	$1 \times 10^{-6} \text{m}^2/\text{s}$
Specific heat $C_p$	813	219	352	$\text{J}/(\text{kg K})$
Thermal effusivity $e_j$	7430	3800	6880	$\text{W} \sqrt{\text{s}}/(\text{m}^2 \text{K})$

temperatures by multiplying it by the transfer function. Then, the sample data can be used to compute the thermal properties of the irradiated layer of the sample through the use of a non-linear curve fit. This is known as the frequency-scan method.

The layered structure of the sample is what enables PTR to measure the thermal properties of the sample. Changes in thermal properties effectively reflect and refract thermal waves much like changes in dielectric constant affect electromagnetic waves. In a layered structure like that shown in Fig. 3, an analytical model can be written which predicts the surface thermal waves for the case of 1D heat propagation, shown in Eqs. (3) through (5). The surface thermal wave  $\Theta$ , is a complex value since the thermal wave number contains the imaginary unit  $i$ , not to be confused with the layer index,  $j$ . Because  $\Theta$  is complex, it represents both the magnitude of the thermal wave and its phase relative to the forcing function of the oscillation (the incident laser). In this model,  $F$  is the mean beam intensity,  $L_j$  is the thickness of each layer, and  $b_{ij}$  is the ratio of the thermal effusivities for layers  $i$  and  $j$  [11]:

$$\Theta_1^{(N)} = \frac{F}{4k_1\sigma_1} \left[ \frac{(1 + R_1)(1 + \rho_{21}^{(N)} e^{-2\sigma_1 L_1})}{1 - R_1 \rho_{21}^{(N)} e^{-\sigma_1 L_1}} \right] \quad (3)$$

$$\rho_{j+1,j}^{(N)} = \frac{(1 - b_{j+1,j}) + \rho_{j+2,j+1}^{(N)} (1 + b_{j+1,j}) e^{-2\sigma_{j+1} L_{j+1}}}{(1 + b_{j+1,j}) + \rho_{j+2,j+1}^{(N)} (1 - b_{j+1,j}) e^{-2\sigma_{j+1} L_{j+1}}} \quad (4)$$

$$\rho_{N,N-1}^{(N)} = \frac{(1 - b_{N,N-1}) + R_N (1 + b_{N,N-1}) e^{-2\sigma_N L_N}}{(1 + b_{N,N-1}) + R_N (1 - b_{N,N-1}) e^{-2\sigma_N L_N}} \quad (5)$$

In these equations,  $N$  is the number of layers in the material, and  $k_j$  is the thermal conductivity of the  $j$ th layer. All subscripts are layer indications, and  $b_{ij}$  is the thermal effusivity of layer  $i$  divided by that of layer  $j$ .  $R_1$  and  $R_N$  are coefficients accounting for heat transfer with the environment. For a surface  $j$ , the  $R$  coefficient can be computed using Eq. (6), where  $h_j$  is convection coefficient:

$$R_j = \frac{k_j \sigma_j - h_j}{k_j \sigma_j + h_j} \quad (6)$$

The environmental heat transfer coefficients for this sample,  $R_1$  and  $R_N$ , were computed to be very nearly one, corresponding to no

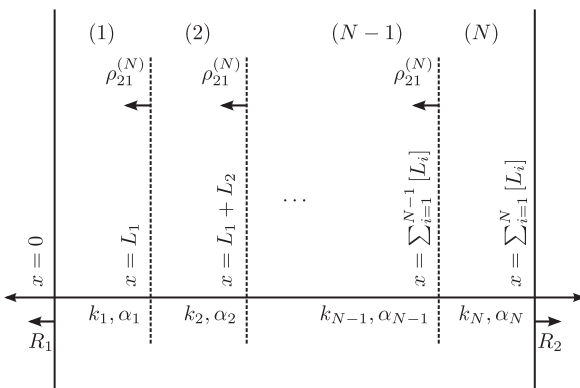


**Fig. 3.** Layered sample structure and nomenclature.

convection from the sample's surfaces. Substituting these values, and actualizing the implicit recursion for a three layer sample Eqs. (3)–(5) are changed into (7)–(9):

$$\Theta_1^{(3)} = \frac{F_0}{2k_1\sigma_1} \left[ \frac{1 + \rho_{21}^{(3)} e^{-2\sigma_1 L_1}}{1 - \rho_{21}^{(3)} e^{-2\sigma_1 L_1}} \right] \quad (7)$$

$$\rho_{21}^{(3)} = \frac{(1 - b_{21}) + \rho_{32}^{(3)} (1 + b_{21}) e^{-2\sigma_2 L_2}}{(1 + b_{21}) + \rho_{32}^{(3)} (1 - b_{21}) e^{-2\sigma_2 L_2}} \quad (8)$$

$$\rho_{32}^{(3)} = \frac{(1 - b_{32}) + (1 + b_{32}) e^{-2\sigma_3 L_3}}{(1 + b_{32}) + (1 - b_{32}) e^{-2\sigma_3 L_3}} \quad (9)$$

A major simplification to the model is used in these equations, since the thermal properties of an irradiated sample actually vary and do not form distinct layers like those normally considered with PTR. By using a three-layer model, the constant variation in properties is simplified to the averages for each region.

This multi-layer model was programmed as a Fortran 95/2003 function and serves as the basis for the curve fit. Experimental data, both from the sample and the glassy carbon, are read into the computer's memory.

A residual function took in the fitting parameters and generated the predicted response using the multi-layer model. The difference between each data point and the model's prediction was computed, and then Gaussian statistics took into account the uncertainties in the data to produce a goodness-of-fit metric. The metrics from all the points were root-sum-squared, producing the full residual.

The residual was minimized using a combination of brute force and the Nelder–Mead simplex method [12]. The fit parameters were each given a range, and a number of points in that range to check. The ranges together make up a search domain and the combinations of the points make up points in that domain which are used as initial guesses to the simplex method. The two-tiered optimization approach ensures that the resulting fit parameters cannot be subject to a bad initial guess. The accuracy of such fit methods has been explored in previous works [13].

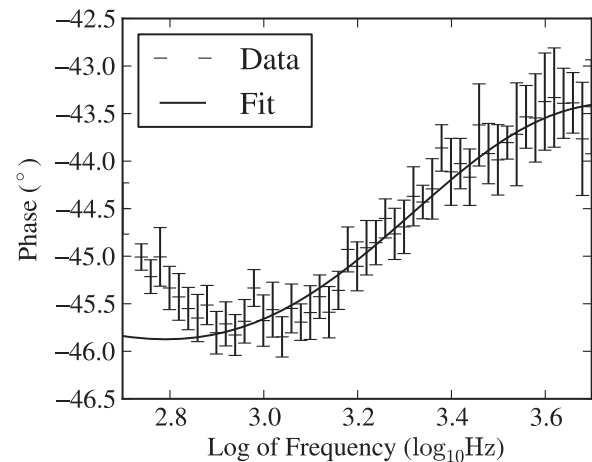


**Fig. 4.** Phase of sample data and curve fit.

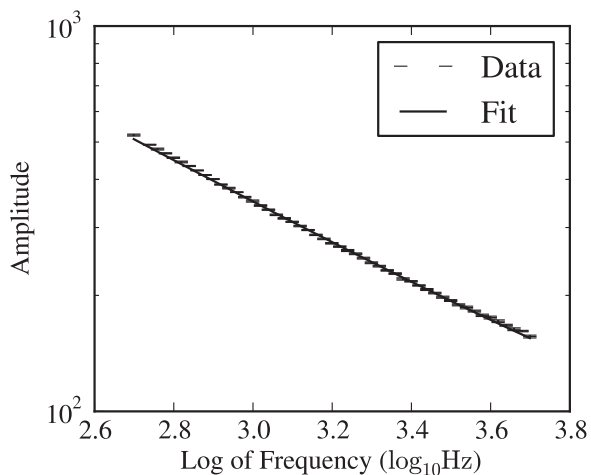


Fig. 5. Amplitude of sample data and curve fit.

The results presented here were computed on a ten processor Beowulf cluster in several hours. The significance of the computation time required for the curve fits is 2-fold. First, the brute-force algorithm which calls the simplex method is easily parallelized, since each range is independent of the others. Second, the computational cost of accurately fitting the heat transfer model for even the one-dimensional case is very high.

## 5. Results

After processing the captured data, the thermal properties of the layer of interest, which has the implanted protons, are summarized in Table 1. The curve fits solved for the thermal diffusivity and effusivity of each layer. Because the density of ZrC has been shown to remain nearly (<0.5%) unchanged by this type of irradiation, from these two properties the thermal conductivity and specific heat may also be computed [8,14]. All values are measured at room temperature.

The curve fit which produced these values is shown along with the sample data in Figs. 4 and 5. The frequencies scanned were selected by first scanning the entire range supported by the PTR system (500–80 kHz), and then using the range with deviation for the curve fit. Both of the fits well-represented the experimental data, although in lower frequencies the phase does not match quite as well. The deviation may be due to three-dimensional effects not considered by the 1D model used for the curve fits.

The calculated thermal conductivity is in agreement with results obtained previously using neutron or ion irradiation by the Oak-Ridge National Laboratory and other studies [17,18]. The other properties are mostly lower than the bulk, which is consistent with thin layers of a material when compared to the same properties for a bulk. The increase in specific heat measured in the first layer is not consistent with measurements done by others on similar ceramics, and suggests that further study is needed [19,2]. The decrease in thermal conductivity in the thin layer is caused by defects in the lattice from the proton bombardment.

## 6. Conclusion

The thermal properties of a ZrC sample were measured and shown to agree with other measured values for similar samples. Although the results are only preliminary, the successful use of PTR for measurement of a prototypical irradiated sample's thermal properties demonstrates the method's effectiveness as a tool for PIE. Small layered samples can be effectively measured without damage or physical contact. These capabilities are well-suited for evaluation of irradiated samples, especially those from nuclear accelerators, because of the small size and layered nature of such samples. Additional measurements of similar samples should be done to better understand how this measurement can be used in the nuclear field.

Further investigation is ongoing, and includes both theoretical and experimental work. The effects of a continuously varying property such as truly exists in the ZrC sample are being considered, as well as the overall uncertainty of a PTR measurement and subsequent calculations from that measurement. A PTR system is being constructed at Utah State University to run measure the properties of more samples like the one considered in this paper.

## Acknowledgements

This work was partially supported by the IMI Program of the National Science Foundation under Award No. DMR 0843934. A. Mandelis is grateful to NSERC for a Discovery Grant. Special thanks go to Yong Yang from the University of Wisconsin for providing the ZrC sample.

## References

- [1] M. Munidasa, M. Tian-Chi, A. Mandelis, S. Brown, L. Mannik, *Materials Science and Engineering A* 159 (1) (1992) 111–118.
- [2] J. Cabrero, F. Audubert, R. Pailler, A. Kusiak, J. Battaglia, P. Weisbecker, *Journal of Nuclear Materials* 396 (2–3) (2010) 202–207.
- [3] A. Mandelis, L. Nicolaidis, Y. Chen, *Physical Review Letters* 87 (2) (2001) 1–4.
- [4] T. Ishiguro, A. Makino, N. Araki, N. Noda, *International Journal of Thermophysics* 14 (1) (1993) 101–121.
- [5] D. Fournier, A. Boccara, *Materials Science and Engineering B* 5 (2) (1990) 83–88.
- [6] G. Crean, M. Somekh, S. Sheard, C. See, *Materials Science and Engineering B* 2 (1–3) (1989) 207–210.
- [7] Y. Nagasaka, T. Sato, T. Ushiku, *Measurement Science and Technology* 12 (2001) 2081.
- [8] Y. Yang, C.A. Dickerson, H. Swoboda, B. Miller, T.R. Allen, *Journal of Nuclear Materials* 378 (2008) 341–348.
- [9] F.A. Modine, T.W. Haywood, C.Y. Allison, *Physical Review B* 32 (1985) 7743–7747, doi:10.1103/physrevb.32.7743, <http://link.aps.org/doi/10.1103/physrevb.32.7743>.
- [10] A. Hellen, A. Matvienko, A. Mandelis, F. Yoav, B.T. Amaechi, *Applied Optics* 49 (2010) 6938–6951.
- [11] A. Mandelis, *Diffusion-Wave Fields: Mathematical Methods and Green Functions*, Springer, 2001.
- [12] D. Olsson, L. Nelson, *Technometrics* 17 (1) (1975) 45–51.
- [13] A. Matvienko, A. Mandelis, S. Abrams, *Applied Optics* 48 (17) (2009) 3193–3204.
- [14] D. Gosset, M. Dolle, D. Simeone, G. Baldinozzi, L. Thome, *Journal of Nuclear Materials* 373 (2008) 123–129.
- [15] A.S. Bolgar, E.A. Guseva, V.V. Fesenko, *Institute of Material Science* 1 (49) (1967) 40–43.
- [16] W. Williams, *JOM, Journal of the Minerals, Metals and Materials Society* 50 (6) (1998) 62–66.
- [17] L. Snead, Y. Katoh, S. Kondo, *Journal of Nuclear Materials* 399 (2010) 200–207.
- [18] S. Gomes, L. David, J. Roger, G. Carlot, D. Fournier, C. Valot, M. Raynaud, *The European Physical Journal Special Topics* 153 (2008) 87–90.
- [19] J.C.C.W. Lee, F.J. Pineau, *Journal of Nuclear Materials* 108 (1982) 678–684.